

PLANT BIOLOGY

Suppression of endogenous gene silencing by bidirectional cytoplasmic RNA decay in *Arabidopsis*

Xinyan Zhang,¹ Ying Zhu,¹ Xiaodan Liu,¹ Xinyu Hong,¹ Yang Xu,² Ping Zhu,² Yang Shen,³ Huihui Wu,¹ Yusi Ji,¹ Xing Wen,¹ Chen Zhang,¹ Qiong Zhao,¹ Yichuan Wang,¹ Jian Lu,^{1,3} Hongwei Guo^{1,3*}

Plant immunity against foreign gene invasion takes advantage of posttranscriptional gene silencing (PTGS). How plants elaborately avert inappropriate PTGS of endogenous coding genes remains unclear. We demonstrate in *Arabidopsis* that both 5'-3' and 3'-5' cytoplasmic RNA decay pathways act as repressors of transgene and endogenous PTGS. Disruption of bidirectional cytoplasmic RNA decay leads to pleiotropic developmental defects and drastic transcriptomic alterations, which are substantially rescued by PTGS mutants. Upon dysfunction of bidirectional RNA decay, a large number of 21- to 22-nucleotide endogenous small interfering RNAs are produced from coding transcripts, including multiple microRNA targets, which could interfere with their cognate gene expression and functions. This study highlights the risk of unwanted PTGS and identifies cytoplasmic RNA decay pathways as safeguards of plant transcriptome and development.

Gene expression and silencing establish the proper transcriptome of eukaryotic cells. Posttranscriptional gene silencing (PTGS), also known as RNA interference, serves as an RNA-based immune system against foreign gene invasion and is engaged in silencing a subset of endogenous genes, mainly transposons (1, 2). PTGS is triggered by cellular double-stranded RNAs, which are subsequently cleaved into 20- to 24-nucleotide (nt) small RNA duplexes by Dicer family proteins (2). One strand of the small RNA duplex can be loaded into an Argonaute (AGO)-containing silencing complex, which targets homologous RNAs for degradation and/or translation inhibition (2). Plants, fungi, and worms possess RNA-dependent RNA polymerases (RDRPs) that could produce secondary small interfering RNA (siRNA) molecules after the primary siRNA targeting, thus amplifying the effects of PTGS (3).

PTGS is an elaborately regulated process. Various plant viruses carry repressors of PTGS, combating plant immunity against infection (4, 5). Several components that participate in mRNA quality control and processing function as repressors of transgene PTGS (6, 7). In this work, we use the model plant *Arabidopsis* to investigate how endogenous protein-coding transcripts avoid being targeted by PTGS machineries that efficiently silence the expression of viral genomes or transgenes.

In *Arabidopsis*, overexpression of ETHYLENE-INSENSITIVE3 (EIN3), a transcriptional activator of ethylene signaling (8), resulted in a small-cotyledon phenotype characteristic of enhanced ethylene response (9) (Fig. 1A) (see also supplementary materials and methods). In a genetic screen searching for suppressors of this stock, we isolated four large-cotyledon mutants that phenocopied the *ein3* loss-of-function mutant (8) (Fig. 1A and fig. S1A). One mutant affected ETHYLENE-INSENSITIVE5 (*EIN5*), encoding a cytoplasmic 5'-3' exoribonuclease known in transgene PTGS repression (7, 10) (fig. S1). The other three mutants (*s28*, *s37*, and *s40*) showed reduced expression of *EIN3* and one of its targets, ETHYLENE-RESPONSE-FACTOR1 (*ERF1*) (11) (Fig. 1B). *s28* carried a mutation in the coding sequence of a DEXH-box RNA helicase (AT3G46960) of the SKI2 (Super-Killer2) type (12) (Fig. 1C and fig. S2A). Green fluorescent protein (GFP)-tagged AtSKI2, expressed exclusively in the cytoplasm (Fig. 1D), restored normal cotyledon development and expression of the *EIN3* transgene in the *s28* line (fig. S3). Two additional *Arabidopsis* insertional *ski2* alleles, *ski2-2* and *ski2-3* (figs. S2A and S4), displayed normal responses to ethylene (fig. S5), excluding AtSKI2 functions in the ethylene signaling pathway. *s37* and *s40*, allelic to each other, both carried nonsense mutations in AtSKI3 (AT1G76630) (12) (Fig. 1C and fig. S2A). In yeast, ScSki2, ScSki3, and ScSki8 function as a cytoplasmic SKI complex to unwind and thread RNAs into the 3'-5' exoribonuclease complex (exosome) for decay (13) (fig. S2B). In *Arabidopsis*, we found peptides characteristic of AtSKI3, AtSKI8, and AtSKI7 and several other proteins associated with AtSKI2 (fig. S6). Pull-down experiments con-

firmed the direct interaction between AtSKI2 and AtSKI3 (Fig. 1E).

Evidence that AtSKI2 is a general repressor of transgene PTGS came from two experiments: (i) When we introduced an unrelated transgene [ADENINE PHOSPHORIBOSYLTRANSFERASE 1 (*APT1*)] to the *ski2-2* line, the phenotype mimicked the *apt1* mutant (14) (fig. S7), suggesting cosuppression of both the *APT1* transgene and endogenous *APT1*. (ii) Mutation of *RDR6*, an RDRP essential for transgene PTGS in plants (15), caused the small-cotyledon phenotype and reactivated expression of the *EIN3* transgene in *s28* (Fig. 1, A and G). Furthermore, the marked accumulation of *EIN3* transgene-derived siRNAs in *s28* was eliminated by *rdr6* mutation (Fig. 1F). Thus, the cytoplasmic 3'-5' and 5'-3' RNA decay pathways mediated by the SKI complex and EIN5, respectively, are required for suppressing transgene PTGS.

Neither cytoplasmic RNA decay pathway alone was essential for plant development, as the *ein5* and *ski2* single mutants were morphologically normal except for mild leaf serrations in *ein5* (10) (Fig. 2A). However, disruption of both pathways (*ein5-1 ski2-2*) proved to be lethal at the embryonic stage (fig. S8A). Hypomorphic *ein5-1 ski2-3* homozygotes (figs. S2A and S4B) were viable but arrested at the early vegetative stage with growth disorders, including defects in meristem, rosette leaves, and leaf coloration (Fig. 2A). *rdr6* rescued the *ein5 ski2* double mutants, and the resultant triple mutants showed normal vegetative growth and fertility (Fig. 2A and fig. S8). Thus, the defects caused by *ein5 ski2* are RDR6-dependent.

We profiled the transcriptomes in the various genotypes. The profile of *rdr6-11 ein5-1 ski2-3* resembled that of *rdr6-11* but differed from that of *ein5-1 ski2-3* (Fig. 2B). We identified 596 differentially expressed genes (111 up-regulated and 485 down-regulated) when both *EIN5* and *AtSKI2* were mutated (fig. S9A). Of the up- and down-regulated genes, 85.6 and 73.0%, respectively, were restored by *rdr6* mutation (fig. S9B), indicating that most of the transcriptomic changes in *ein5-1 ski2-3* are dependent on RDR6.

The genes regulated by the combination of *EIN5* and *AtSKI2* are enriched in functional categories such as flavonoid biosynthesis, ribosome, and photosynthesis (table S1). For instance, expression of several anthocyanin biosynthesis enzymes (DFR, TT8) and their regulatory transcription factors (PAP1, PAP2) (16) was up-regulated in *ein5-1 ski2-3* but reduced in *rdr6-11 ein5-1 ski2-3* (Fig. 2C). Accordingly, anthocyanin highly accumulated in *ein5-1 ski2-3* but not in *rdr6-11 ein5-1 ski2-3* (Fig. 2D), manifesting as purple pigmentation in rosette leaves of *ein5-1 ski2-3* plants (Fig. 2A).

The defects of *ein5 ski2* were rescued by other mutations that affect the 21- to 22-nt siRNA pathway, such as *ago1*, *suppressor of gene silencing3* (*sgs3*), and the *dicer-like4* (*dcl4*) *dcl2* double mutant (17) (Fig. 3, A and B, and figs. S10 and S11). In *Arabidopsis*, *DCL4* generates 21-nt

¹State Key Laboratory of Protein and Plant Gene Research, College of Life Sciences, Peking University, Beijing 100871, China. ²Biodynamic Optical Imaging Center, School of Life Sciences, Peking University, Beijing 100871, China.

³Peking-Tsinghua Center for Life Sciences, Peking University, Beijing 100871, China.

*Corresponding author. E-mail: hongweig@pku.edu.cn

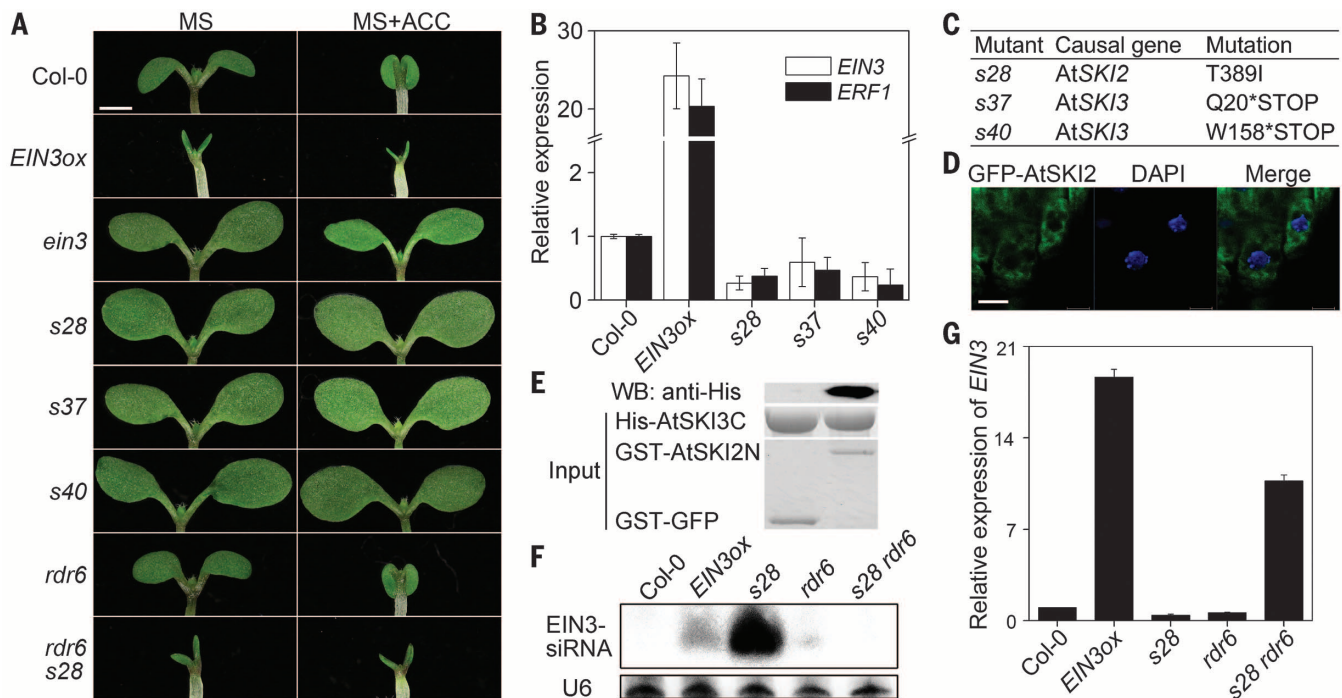


Fig. 1. RDR6-dependent transgene PTGS upon the dysfunction of 3'-5' RNA decay. (A) Cotyledon phenotype of 6-day-old seedlings grown on Murashige and Skoog (MS) medium supplemented with or without 10 μ M ACC, an ethylene biosynthetic precursor. s28, s37, and s40 mutants were generated in the *EIN3ox* (*EIN3*-overexpressor) background. The s28 *rdr6* double mutant was generated by crossing. Scale bar, 1 mm. (B) Relative expression levels of *EIN3* and its target gene *ERF1* in 6-day-old seedlings. Error bars indicate SD; number of replicates (n) = 3. (C) Identification of the causal

genes in the mutants by positional cloning. Mutations of amino acid (aa) residues are indicated. T, Thr; I, Ile; Q, Gln; W, Trp. (D) Subcellular localization of AtSKI2 fused with GFP. 4',6-diamidino-2-phenylindole (DAPI) staining indicates the nuclei. Scale bar, 5 μ m. (E) In vitro glutathione S-transferase (GST) pull-down assay between the C terminus of AtSKI3 (AtSKI3C, aa 930 to 1169) and the N terminus of AtSKI2 (AtSKI2N, aa 1 to 344). WB, Western blotting. (F) Northern blot detection of small RNAs derived from *EIN3*. (G) Relative expression levels of *EIN3* in 6-day-old seedlings. Error bars indicate SD; n = 3.

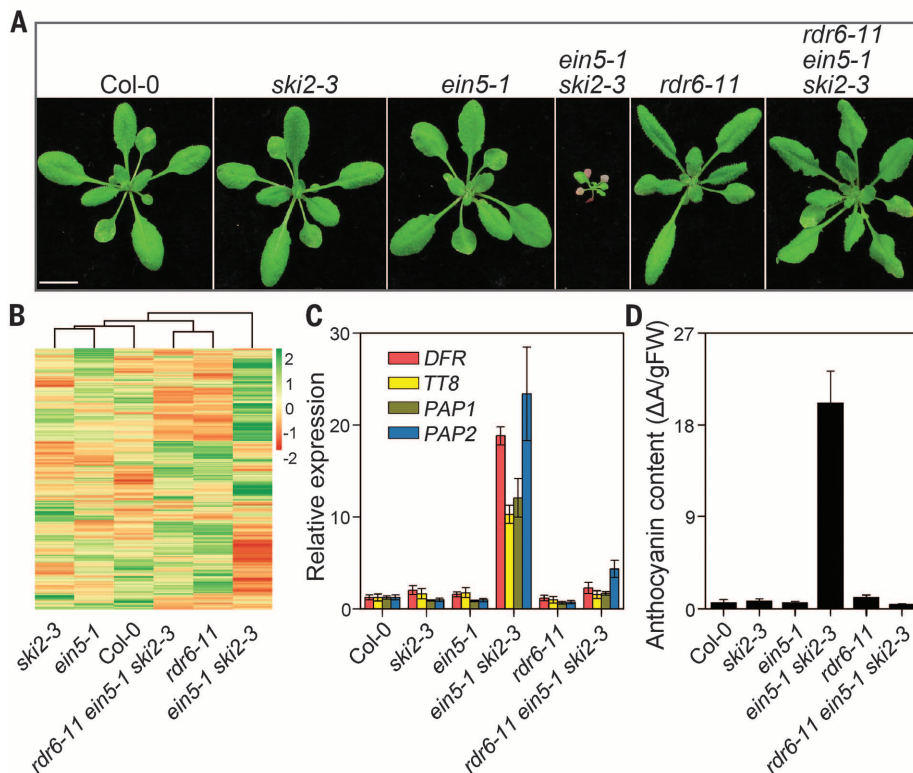


Fig. 2. Disruption of bidirectional RNA decay exhibits RDR6-dependent developmental defects and transcriptomic alterations. (A) Rosette morphology of 3-week-old plants of indicated genotypes. Scale bar, 1 cm. (B) Clustering of transcriptome profiles of *ein5-1*, *ski2-3*, *rdr6-11*, and their combinations. The clustering results are based on expression levels of 15,663 genes that have the expression levels with reads per kilobase per million > 1 in the Col-0 background. (C) Relative expression of genes that regulate anthocyanin biosynthesis in 16-day-old plants. Error bars indicate SD; n = 3. (D) Quantification of anthocyanin accumulation in 16-day-old plants. Error bars indicate SD, n = 6.

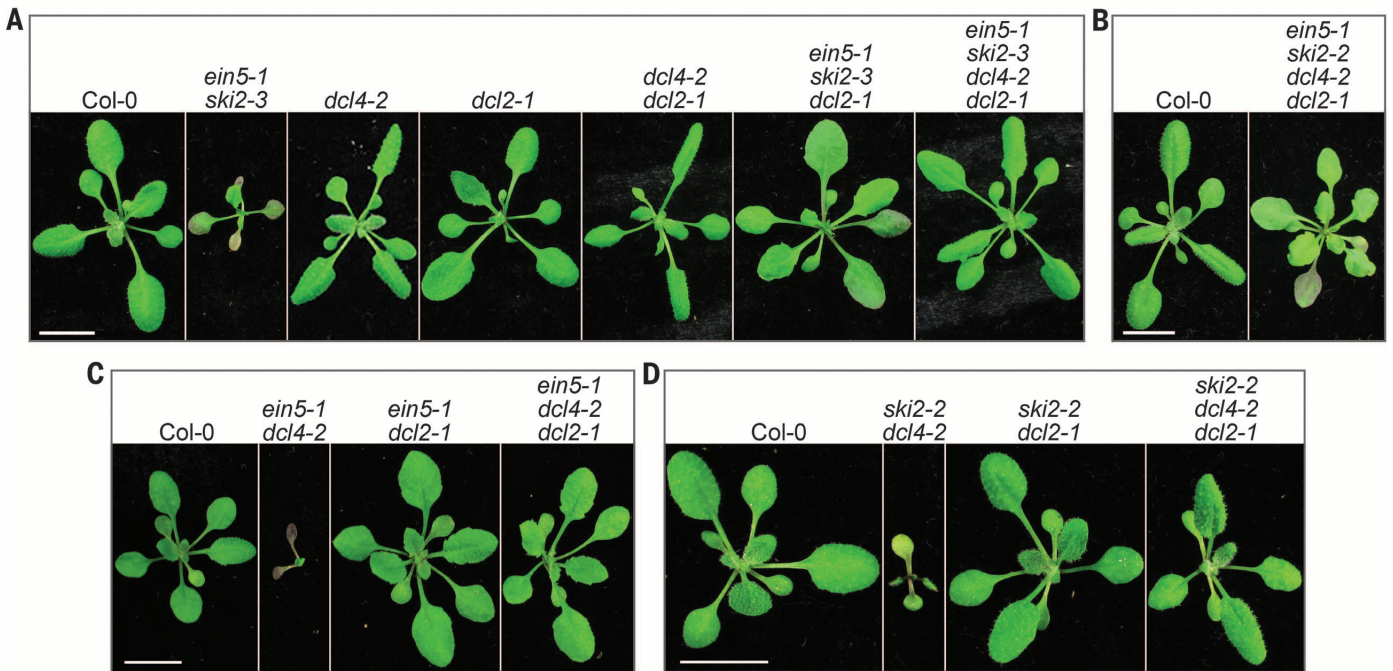


Fig. 3. Genetic interaction between the PTGS and RNA decay pathways. (A to D) Rosette morphology of 19-day-old plants was shown. No *ein5-1 ski2-3 dcl4-2* plant was viable based on genotyping the segregating population derived from the *ein5-1 ski2-3* hemizygote and *dcl4-2 dcl2-1* cross (A). Similarly, the *ein5-1 ski2-2* double mutants were not viable, and by genotyping the F₂ and F₃ plants propagated from the *ein5-1 ski2-2* hemizygote and *dcl4-2 dcl2-1* cross, no *ein5-1 ski2-2 dcl2-1* or *ein5-1 ski2-2 dcl4-2* triple mutants were viable (B). Scale bars, 1 cm.

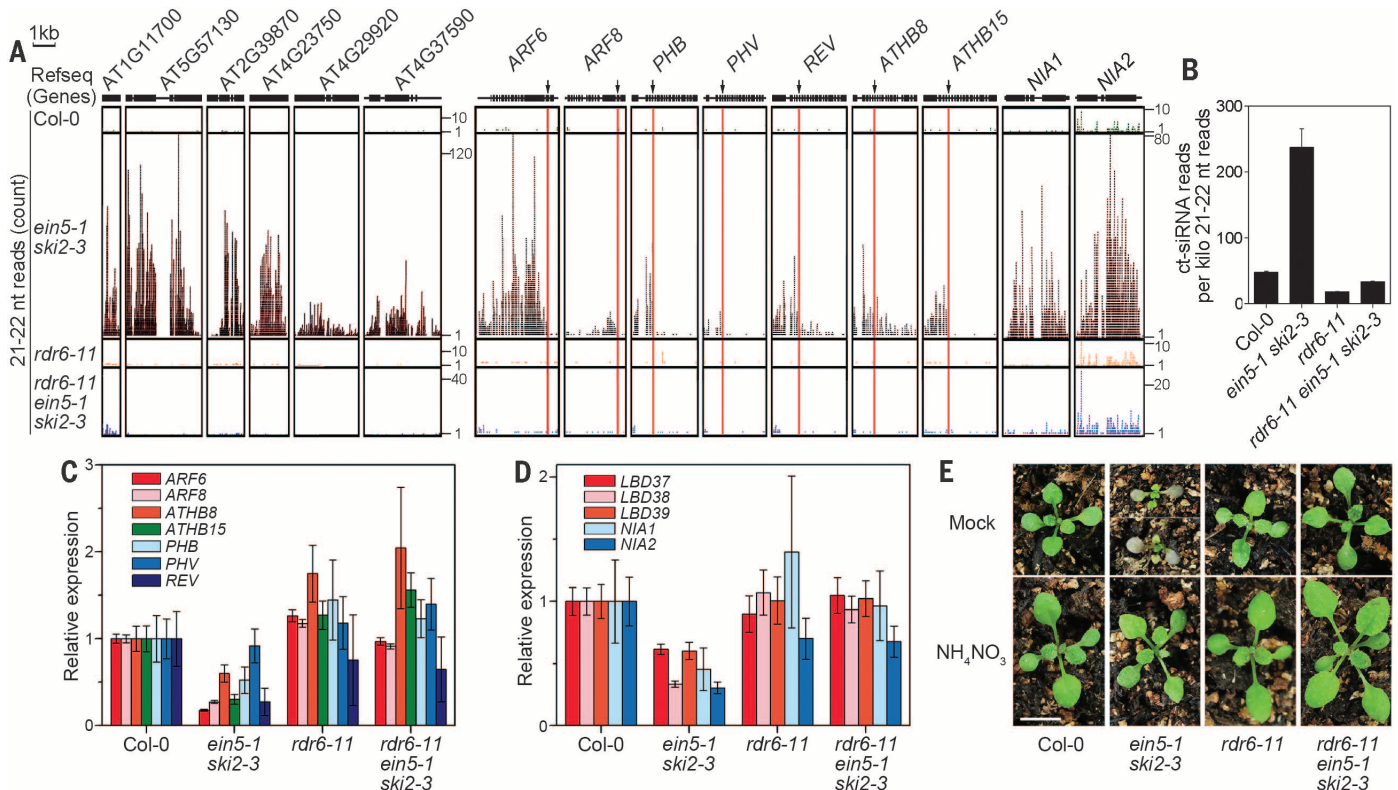


Fig. 4. Identification and functional analysis of a class of siRNAs accumulated in *ein5 ski2*. (A) Accumulation of 21- to 22-nt siRNAs derived from representative coding genes in *ein5 ski2*, but barely in other genotypes. Arrows indicate the miRNA cleavage sites in the selected miRNA-target genes. (B) Overall abundance of ct-siRNAs generated from 441 protein-coding loci in each genotype. Error bars indicate SD; *n* = 3. (C) Relative

expression levels of select miRNA target genes (*ARF* and *HD-ZIPIII* family genes). Error bars indicate SD; *n* = 3. (D) Relative expression levels of *NIA1/2* and three nitrogen-responsive genes (*LBD37*, -38, and -39). Error bars indicate SD; *n* = 3. (E) Two-week-old plants grown in soil irrigated with water (Mock) or 1.65 g/liter ammonium nitrate solution (NH₄NO₃). Scale bar, 1 cm.

siRNAs, whereas DCL2 generates 22-nt siRNAs, which could efficiently trigger secondary siRNA biogenesis (18). Neither *dcl2* nor *dcl4* rescued the lethality of *ein5-1 ski2-2* (Fig. 3B); however, *dcl2* evidently recovered the developmental disorders of the hypomorphic *ein5-1 ski2-3* (Fig. 3A). Thus, both 21- and 22-nt siRNA pathways are deleterious to plant survival, and the 22-nt siRNA pathway is particularly detrimental to plant development when bidirectional RNA decay is disrupted. In contrast to normal morphology of *ein5 dcl2* and *ski2 dcl2*, both *ein5 dcl4* and *ski2 dcl4* plants displayed defects in rosette growth, meristem function, and leaf pigmentation. Further loss of DCL2 function rescued these defects (Fig. 3, C and D). Thus, upon deficiency of either 5' (EIN5) or 3' (AtSKI2) RNA decay, the DCL4-mediated pathway could compete with the DCL2-mediated pathway to minimize the risk that 22-nt siRNAs might trigger amplified PTGS harmful to plant development.

We used small RNA sequencing to profile small RNA production in wild-type (Col-0), *rdr6-11*, *ein5-1 ski2-3*, and *rdr6-11 ein5-1 ski2-3* (fig. S12A). We found that few reads mapped to all eight *Arabidopsis TAS* genes in *rdr6-11* and *rdr6-11 ein5-1 ski2-3*, consistent with the requirement of RDR6 for trans-acting siRNA (tasiRNA) biogenesis (19). Abundant and comparable levels of tasiRNA were detected in Col and *ein5-1 ski2-3* for 7 *TAS* genes (fig. S12, B and C), except for *TAS4* tasiRNAs, which may have accumulated due to the elevated expression of *TAS4* in *ein5-1 ski2-3* (fig. S13). Therefore, defects in cytoplasmic RNA decay do not affect tasiRNA biogenesis.

To further explore the genetic cause of detrimental PTGS, we filtered the genes that generate 21- to 22-nt siRNAs using two criteria: (i) loci with more mapping reads of siRNAs in *ein5-1 ski2-3* than in Col [twofold cutoff, $P < 0.005$, false discovery rate (FDR) < 0.1], and (ii) loci with fewer mapping reads of siRNAs in *rdr6-11 ein5-1 ski2-3* than in *ein5-1 ski2-3* (twofold cutoff, $P < 0.005$, FDR < 0.1). Of 456 genes that met these criteria, 441 encoded proteins (Fig. 4, A and B, and table S2). We named the siRNAs derived from the 441 loci as coding transcript-derived siRNAs (ct-siRNAs). Among these 441 loci were 39 microRNA (miRNA)-targeted protein-coding genes (table S3), including miR167 targets (*ARF6*, *ARF8*) and miR165/166 targets (five *HD-ZIP III* genes) (Fig. 4A and fig. S14). ct-siRNAs arise from either 5' miRNA-cleavage fragments or 5' plus 3' fragments of these miRNA targets (Fig. 4A and fig. S15), distinct from the biogenesis of most tasiRNAs within 3' fragments of *TAS* loci (20).

The ct-siRNA loci were overrepresented in the down-regulated genes of *ein5-1 ski2-3* (fig. S16). For instance, expression of the above-mentioned *ARF6/8* and *HD-ZIP III* genes was reduced in *ein5-1 ski2-3* but not in *rdr6-11 ein5-1 ski2-3* (Fig. 4C), suggesting that the RDR6-dependent ct-siRNA biogenesis intensifies the repression of gene expression triggered by miRNAs. We identified *NIA1* and *NIA2*, which encode two

nitrate reductases required for nitrate assimilation in *Arabidopsis* (21), from the top 20 loci that show the most notable ct-siRNA production in *ein5 ski2* (Fig. 4A and fig. S17). Expression of *NIA1* and *NIA2*, as well as three nitrogen-responsive genes (*LBD37*, *-38*, and *-39*) (22), was reduced in *ein5-1 ski2-3* and was restored in *rdr6-11 ein5-1 ski2-3* (Fig. 4D). Thus, ct-siRNA-mediated silencing of *NIA1* and *NIA2* genes disturbed nitrogen metabolism, which activates anthocyanin biosynthesis (23). In agreement, the purple pigmentation of *ein5-1 ski2-3* leaves at the early stage was normalized when the plants were irrigated with ammonium nitrate, which compensates for the compromised nitrate assimilation (Fig. 4E). Thus, biogenesis of ct-siRNAs in many cases could reduce the expression of their cognate genes and compromise gene functions.

The ct-siRNA loci were also overrepresented in the up-regulated genes of *ein5-1 ski2-3* (fig. S16). Furthermore, the ct-siRNA loci, on average, were expressed at markedly higher levels than the rest of the genome (fig. S18). Transgenes expressed at higher levels are more likely to undergo PTGS to produce siRNA (24). It is thus likely that accumulation of a subset of ct-siRNAs reflects the disturbed expression of their cognate genes upon dysfunction of RNA decay pathways. In line with this, *TAS4*-tasiRNA accumulated to high levels due to elevated expression of the *TAS4* gene in *ein5 ski2* (figs. S12C and S13).

Here we describe a class of endogenous siRNAs (ct-siRNAs) with these characteristics: (i) 21 or 22 nt in length; (ii) derived from coding transcripts; (iii) produced upon the dysfunction of EIN5- and AtSKI-mediated RNA decay; (iv) dependent on RDR6, SGS3, DCL2, and DCL4 for biogenesis; and (v) partially dependent on AGO1 for action (fig. S19). Our study reveals that both transgene and endogenous PTGS occurs upon dysfunction of bidirectional cytoplasmic RNA decay, which normally eliminates aberrant transcripts arising from RNA degradation, end processing, or endo-cleavage (25). When RNA decay pathways are disrupted by genetic mutation or overloaded by overexpression of foreign genes, aberrant transcripts are selected and channeled into PTGS pathways to produce 21- to 22-nt ct-siRNAs. The DCL4-mediated pathway could serve as a decoy to antagonize the more destructive DCL2-mediated pathway, protecting endogenous mRNAs from undesirable clearance (fig. S19). Thus, cytoplasmic RNA decay sets a silencing threshold such that those invading or vastly expressed genes with high levels of aberrant RNA production probably undergo PTGS, whereas the majority of endogenous genes hardly do. As such, the siRNA-based defense system in plants that originally evolved against genome invasion carries risks of triggering adverse endogenous PTGS not typical of the protein-based immune systems found in vertebrates (3). We also propose that cytoplasmic RNA decay and siRNA pathways act as crucial components in the miRNA regulatory network. After an ini-

tial miRNA-directed cleavage, cytoplasmic RNA decay could preclude sustained or exacerbated siRNA-triggered silencing of target gene expression. Notably, miRNA-triggered tasiRNA biogenesis seems not to be affected by cytoplasmic RNA decay, raising the question as to how aberrant transcripts are sorted and targeted between cytoplasmic RNA decay and PTGS pathways.

REFERENCES AND NOTES

- C. Cogoni, G. Macino, *Curr. Opin. Genet. Dev.* **10**, 638–643 (2000).
- R. C. Wilson, J. A. Doudna, *Annu. Rev. Biophys.* **42**, 217–239 (2013).
- M. Ghildiyal, P. D. Zamore, *Nat. Rev. Genet.* **10**, 94–108 (2009).
- M. Incarbone, P. Dunoyer, *Trends Plant Sci.* **18**, 382–392 (2013).
- N. Pumplin, O. Voinnet, *Nat. Rev. Microbiol.* **11**, 745–760 (2013).
- A. B. Moreno *et al.*, *Nucleic Acids Res.* **41**, 4699–4708 (2013).
- S. Gazzani, T. Lawrenson, C. Woodward, D. Headon, R. Sablowski, *Science* **306**, 1046–1048 (2004).
- Q. Chao *et al.*, *Cell* **89**, 1133–1144 (1997).
- H. Guo, J. R. Ecker, *Cell* **115**, 667–677 (2003).
- G. Olmedo *et al.*, *Proc. Natl. Acad. Sci. U.S.A.* **103**, 13286–13293 (2006).
- R. Solano, A. Stepanova, Q. Chao, J. R. Ecker, *Genes Dev.* **12**, 3703–3714 (1998).
- E. Dorcey *et al.*, *PLOS Genet.* **8**, e1002652 (2012).
- J. T. Brown, X. Bai, A. W. Johnson, *RNA* **6**, 449–457 (2000).
- X. Zhang *et al.*, *Mol. Plant* **6**, 1661–1672 (2013).
- T. Dalmay, A. Hamilton, S. Rudd, S. Angell, D. C. Baulcombe, *Cell* **101**, 543–553 (2000).
- E. Grotewold, *Annu. Rev. Plant Biol.* **57**, 761–780 (2006).
- N. G. Bologna, O. Voinnet, *Annu. Rev. Plant Biol.* **65**, 473–503 (2014).
- F. Vazquez, T. Hohn, *Scientifica* **2013**, 783253 (2013).
- A. Peragine, M. Yoshikawa, G. Wu, H. L. Albrecht, R. S. Poethig, *Genes Dev.* **18**, 2368–2379 (2004).
- E. Allen, Z. Xie, A. M. Gustafson, J. C. Carrington, *Cell* **121**, 207–221 (2005).
- C. F. Hwang, Y. Lin, T. D'Souza, C. L. Cheng, *Plant Physiol.* **113**, 853–862 (1997).
- G. Rubin, T. Tohge, F. Matsuda, K. Saito, W. R. Scheible, *Plant Cell* **21**, 3567–3584 (2009).
- C. Diaz *et al.*, *Plant Cell Physiol.* **47**, 74–83 (2006).
- D. Schubert *et al.*, *Plant Cell* **16**, 2561–2572 (2004).
- C. A. Beelman, R. Parker, *Cell* **81**, 179–183 (1995).

ACKNOWLEDGMENTS

We thank Y. Qi (Tsinghua University) and F. Tang and Y. Li (Peking University) for assistance in RNA sequencing experiments. We also thank J. Olson (Peking University) for assistance in English editing. This work is supported by the National Basic Research Program of China (973 Program; grant 2012CB910902) and the National Natural Science Foundation of China (grants 91217305 and 91017010 to H.G.). The publication fee is covered by the 111 Project of Peking University. Data have been deposited in the Gene Expression Omnibus under accession numbers GSE52407 and GSE57936. The supplementary materials contain additional data.

SUPPLEMENTARY MATERIALS

www.sciencemag.org/content/348/6230/120/suppl/DC1
Materials and Methods
Figs. S1 to S19
Tables S1 to S4
References (26–45)

9 November 2014; accepted 27 February 2015
10.1126/science.aaa2618

This copy is for your personal, non-commercial use only.

If you wish to distribute this article to others, you can order high-quality copies for your colleagues, clients, or customers by [clicking here](#).

Permission to republish or repurpose articles or portions of articles can be obtained by following the guidelines [here](#).

The following resources related to this article are available online at www.sciencemag.org (this information is current as of November 18, 2015):

Updated information and services, including high-resolution figures, can be found in the online version of this article at:

<http://www.sciencemag.org/content/348/6230/120.full.html>

Supporting Online Material can be found at:

<http://www.sciencemag.org/content/suppl/2015/04/01/348.6230.120.DC1.html>

This article **cites 44 articles**, 23 of which can be accessed free:

<http://www.sciencemag.org/content/348/6230/120.full.html#ref-list-1>

This article has been **cited by 2** articles hosted by HighWire Press; see:

<http://www.sciencemag.org/content/348/6230/120.full.html#related-urls>

This article appears in the following **subject collections**:

Botany

<http://www.sciencemag.org/cgi/collection/botany>